

Formation of H₂-rich iodine-hydrogen compounds at high pressureHPSTAR
506-2018Jack Binns,¹ Philip Dalladay-Simpson,¹ Mengnan Wang,¹ Graeme J. Ackland,² Eugene Gregoryanz,^{1,2,3} and Ross T. Howie¹¹Center for High Pressure Science Technology Advanced Research, Shanghai, People's Republic of China²Centre for Science at Extreme Conditions and School of Physics and Astronomy,
University of Edinburgh, Edinburgh EH9 3JZ, United Kingdom³Key Laboratory of Materials Physics, Institute of Solid State Physics, Chinese Academy of Sciences, Hefei, People's Republic of China

(Received 16 November 2017; published 24 January 2018)

We have used synchrotron x-ray and Raman spectroscopic studies combined with molecular dynamics to investigate the I₂-H₂ system at high pressure. By laser heating the mixture above 25 GPa we synthesized the molecular compound HI(H₂)₁₃, with the AB₁₃ structure type and unusually high volumetric hydrogen content. The isolation of HI molecules by (H₂)₁₃ supramolecular clusters stabilizes the compound over a remarkable pressure range from 9 to at least 130 GPa. At lower pressures and 300 K another compound, hydrogen diiodane H₂(HI)₂, spontaneously forms, being stable up to 12.5 GPa.

DOI: [10.1103/PhysRevB.97.024111](https://doi.org/10.1103/PhysRevB.97.024111)

I. INTRODUCTION

Molecular hydrogen has been the focus of intense research for several decades, both as a possible energy carrier and as a subject of fundamental studies into its behavior under extremes of temperature and pressure [1–5]. Extreme-conditions research has revealed the potential of molecular clathrates and metal-organic frameworks to act as hydrogen-storage materials, while the claim of high-temperature superconductivity in H₂S has reignited the interest in dense hydrogen-bearing materials [6–9]. Another element, iodine (I₂), an archetypal diatomic molecular system, has been predicted to exhibit physical phenomena and phase transitions similar to hydrogen but at much lower pressures. Indeed, some of these phenomena and transformations have been experimentally observed [10–12]. Therefore the high-pressure behavior of hydrogen-iodine mixtures might reveal some new and interesting physics. For instance, structure-searching calculations have suggested that compounds of hydrogen (H₂) and iodine (I₂) with various stoichiometries could be stable at pressures above 30 GPa, with superconducting phases emerging above 100 GPa with *T_c* up to 18 K [13,14].

However, experimental studies of the high-pressure behavior of hydrogen iodide (HI) have been hindered by its intrinsic instability due to the rapid decrease of HI intermolecular distances with increasing density and therefore the decomposition of the HI molecules at pressure [15] and, to a lesser extent, due to the sensitivity of HI to diagnostic techniques such as laser or x-ray beams. Recent work has shown that at room temperature in a matrix of hydrogen, HI still decomposes at 10 GPa, while cooling further stabilizes HI to about 20 GPa at 80 K [15]. Although theoretical predictions also find HI to be unstable with respect to decomposition, they predict the hydrogen-rich compounds HI(H₂)₂, H₂I, and (H₂)₂I to be more stable, but they have not been observed experimentally [13,14].

Herein we report on the synthesis and stability of hydrogen-iodine compounds under pressure through x-ray diffraction and Raman spectroscopy combined with laser-heating techniques and molecular dynamics calculations. At pressures above

25 GPa, laser heating the mixture of metallic iodine and molecular H₂ promotes the synthesis of supramolecular HI(H₂)₁₃, which adopts the AB₁₃ structure, known to be stable for binary hard-sphere packing with size ratios of around 0.558 [16]. This structural type has been observed in a wide range of systems but never before in a molecular configuration at high pressure. The icosahedral clusters of H₂ molecules isolate the HI molecule, resulting in an extreme stability range, from 9 to at least 130 GPa. By compressing HI-H₂ mixtures at 300 K, we observe the formation of another molecular compound, H₂(HI)₂, which exhibits stability similar to that of pure HI [15]. We note that previous theoretical structure searches identifying several H₂-HI stoichiometries have not considered such extreme H₂ contents as we report here [13,14].

II. METHODS

Mixtures of HI-H₂ were synthesized in diamond-anvil cells by the direct reaction between solid I₂ and H₂. Various concentrations of I₂ were loaded in an Ar-atmosphere glove box. High-purity (99.9%) H₂ was subsequently gas loaded at 0.2 GPa. For pressures below 50 GPa, a small chip of ruby or gold was included as a pressure calibrant and cross-checked against the equation of state of I₂ during analysis [17,18]. For samples above 50 GPa, no additional marker was used, and pressure was determined by Raman spectroscopy of the stressed diamond edge [19]. After loading, samples were then irradiated with 200 mW of 532-nm laser light to photodissociate I₂, which reacts vigorously with H₂, producing a mixture of liquid HI and H₂ showing clear phase separation. Samples were left for 24 h to equilibrate, after which there was a mixture of H₂ and HI, with trace amounts of I₂. By varying the initial quantity of I₂ we were able to control the mixture ratio of HI and H₂.

In situ laser heating was carried out on mixtures of solid I₂ and H₂ in diamond-anvil cells at pressures of at least 20 GPa. Samples for x-ray diffraction data collection were then compressed to 20 and 33 GPa before irradiation with up to 50 W of 1064-nm laser light. We estimate temperatures to

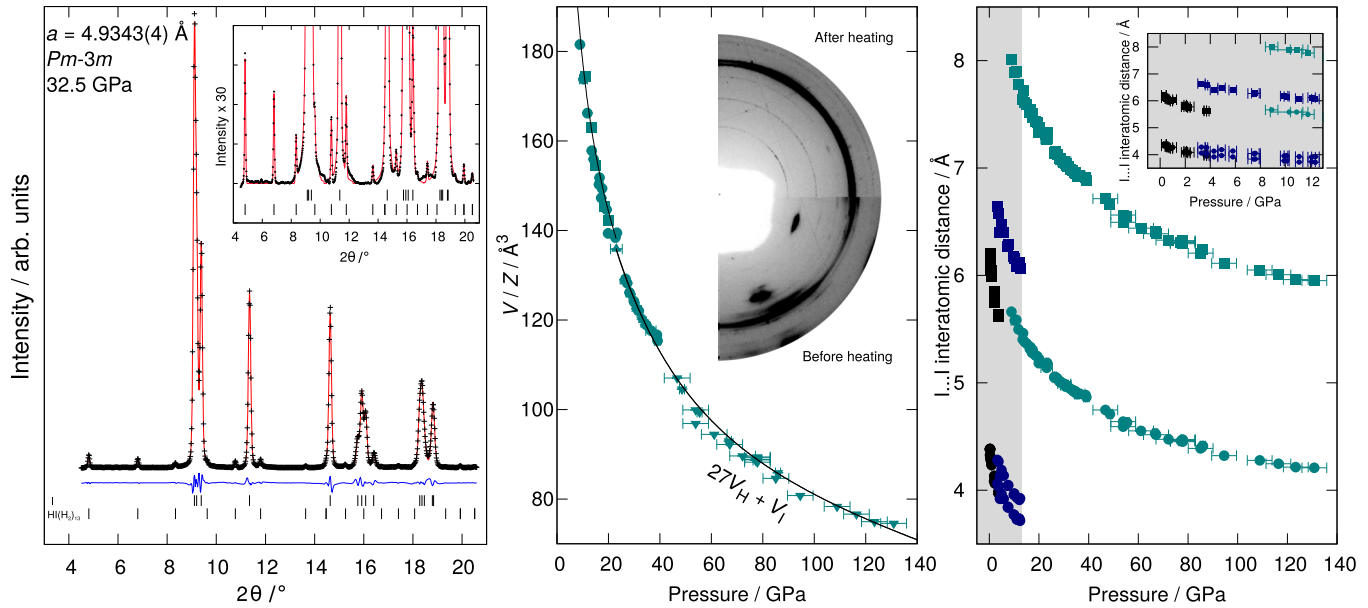


FIG. 1. X-ray diffraction structure analysis of $\text{HI}(\text{H}_2)_{13}$. Left: High-pressure x-ray diffraction pattern collected from a laser-heated mixture of H_2 and I_2 at 32.5 GPa ($\lambda = 0.4141 \text{ \AA}$). Tick marks indicate Bragg peaks due to $\text{I}_2\text{-II}$ (top) and $\text{HI}(\text{H}_2)_{13}$ (bottom). The inset shows the same patterns with intensities scaled times 30 to highlight the peaks due to $\text{HI}(\text{H}_2)_{13}$. Middle: $\text{HI}(\text{H}_2)_{13}$ equation of state; symbols are experimental data from individual runs. The solid line corresponds to volume derived from the atomic equations of state of iodine and hydrogen. The inset shows x-ray diffraction patterns before and after laser heating. The well-defined rings at a low angle are due to $\text{HI}(\text{H}_2)_{13}$. Right: Changes in nearest and next-nearest $\text{I}\cdots\text{I}$ distances with pressure in HI (black), $\text{H}_2(\text{HI})_2$ (dark blue), and $\text{HI}(\text{H}_2)_{13}$ (green). The low-pressure region is shown in the inset.

be less than 1000 K as no blackbody radiation was detectable from the sample during heating. These pressures were chosen to determine if the molecular dissociation of I_2 , occurring between 23.2 and 30.4 GPa, influenced the reactivity of I_2 . These pressures are also high enough to ensure the full decomposition of HI and $(\text{HI})_2\text{H}_2$ into their constituent elements [15].

Samples were characterized by microfocused x-ray diffraction and Raman spectroscopy. X-ray diffraction data were collected at beamlines BL10XU, SPring-8, Japan, and 16-ID-B, Advanced Photon Source, United States, using incident energies of ~ 30 keV. Two-dimensional image-plate data were integrated with DIOPTAS [20] to yield intensity vs 2θ plots. Le Bail profile refinement was carried out in JANA2006 [21], and refinement of the crystal structure was carried out against $|F^2|$ with the SHELXL refinement package [22]. X-ray diffraction and Raman spectroscopy measurements prior to laser heating indicate the cell contained pure I_2 , H_2 , and the Au pressure marker.

Ab initio molecular dynamics calculations were done using density functional theory and the CASTEP program [23] with the Perdew-Burke-Ernzerhof exchange correlation and on-the-fly iodine pseudopotential. For a detailed description of the experimental and theoretical methods used in this study see the Supplemental Material [24].

III. RESULTS AND DISCUSSION

At low pressures (0.2–0.5 GPa) H_2 and I_2 react spontaneously. Once synthesized, HI is very unstable on compression and decomposes by ~ 10 GPa at 300 K [15]. On further compression to 60 GPa at 300 K, there is no further reaction

between I_2 and H_2 . High-temperature laser heating has been shown to be an effective way to synthesize high-pressure compounds with unusual stoichiometries [25,26]. By performing *in situ* laser-heating x-ray diffraction measurements at pressures of ≥ 24 GPa we observe the appearance of relatively weak but well defined diffraction lines in addition to those from iodine (Fig. 1). Interestingly, these lines appear only upon quenching to room temperature. These diffraction lines could be readily indexed to a primitive cubic unit cell ($a = 5.080(1) \text{ \AA}$ at 25 GPa). Initial analysis of the diffraction data indicated a single, strong, electron-density peak corresponding to HI , arranged in a primitive cubic lattice. The spacing between HI molecules (i.e., unit-cell length a) was clearly much larger than the combined radii of HI , suggesting the presence of additional H_2 molecules.

Raman spectroscopic measurements confirmed two distinct molecular species in the compound with two characteristic intramolecular vibrational modes (vibrons), one mode at $\sim 2300 \text{ cm}^{-1}$ due to HI molecules and one peak due to H_2 molecules at approximately 4220 cm^{-1} [at 20 GPa; see Fig. 2(a)]. Measuring the vibrational modes as a function of pressure shows that both vibrons exhibit a turnover in frequency, with maxima at a pressure of 25 GPa. Both vibrational modes are observable up to 60 GPa, the highest pressure achieved in the Raman study, and show considerable broadening and reduction in intensity with increasing pressure (Fig. S1 [24]). We were not able to discern any distinctive modes in the low-frequency regime due to the strong Raman bands from the unreacted iodine. On decompression at 300 K, the compound is found to be stable to 9 GPa, below which there is the simultaneous disappearance of the corresponding

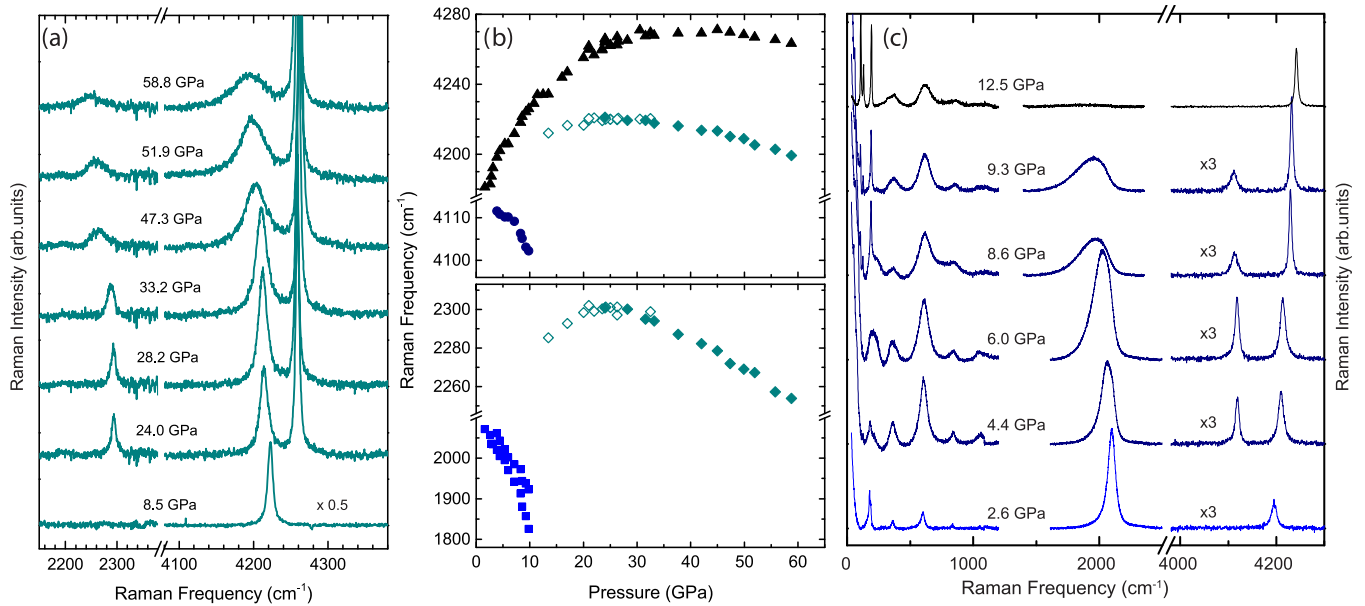


FIG. 2. Representative Raman spectra and vibrational mode positions of $\text{HI}(\text{H}_2)_{13}$ and $\text{H}_2(\text{HI})_2$. (a) Representative Raman spectra from a sample containing $\text{HI}(\text{H}_2)_{13}$ and pure H_2 on compression and decompression. (b) Vibrational frequencies vs pressure of HI (light blue squares), $\text{H}_2(\text{HI})_2$ (dark blue circles), $\text{HI}(\text{H}_2)_{13}$ (green diamonds), and H_2 (black triangles) at 300 K. Solid symbols represent data on compression, while open symbols represent data collected on decompression. (c) Representative Raman spectra of the $\text{HI}-\text{H}_2-\text{I}_2$ mixture (light blue), formation of $\text{H}_2(\text{HI})_2$ at 3.9 GPa (dark blue), and its subsequent decomposition with pressure (black).

vibrational modes and diffraction lines, leaving signals from only I_2 and H_2 .

To estimate the stoichiometry of this compound, we compare the experimentally determined volume per formula unit with that calculated for various compositions derived from the atomic equations of state for I_2 [11,27] and H_2 [28]. As can be seen in Fig. 1, a composition of $\text{HI}(\text{H}_2)_{13}$ results in a close fit to the observed equation of state. Structures with composition AB_{13} have been observed in a number of systems: from intermetallic compounds to binary colloidal crystals and Brazilian gem opals [29–31]. Two forms of AB_{13} structure are known and differ by the arrangement of B spheres, which may form icosahedra or cuboctahedra around a central B sphere with corresponding space-group symmetries $Fm\bar{3}c$ and $Pm\bar{3}m$ [31]. Hydrogen is a poor scatterer of x rays, ruling out direct determination of the H_2 arrangement by x-ray diffraction methods. To distinguish between the two packing types we have performed molecular dynamics (MD) density functional theory calculations at 300 K and 30 GPa. Figure 3(a) shows an instantaneous snapshot and averaged atomic positions over 5 ps. At this pressure H_2 and HI molecules exhibit extensive rotational disorder but are stable and do not undergo proton transfer. The average positions from the simulation clearly show H_2 molecules adopting an icosahedral distribution as found in the $Fm\bar{3}c$ polymorph [see Fig. 3(a)]. Fivefold symmetry is incompatible with translational symmetry, so in the derived crystal structure alternate icosahedra are rotated 90° relative to each other, resulting in a cubic structure containing eight $(\text{H}_2)_{13}$ units in the $Fm\bar{3}c$ conventional cell [Fig. 3(b)].

A single HI vibron is in agreement with one unique HI molecular environment. The appearance of the vibron is consistent with rotational disorder as in HI phase I [15,32]. As shown in Fig. 3, there are two unique H_2 molecular

environments present in the AB_{13} structure (see Ref. [24]), however we are unable to distinguish between these modes, within the icosahedra, using Raman spectroscopy. The $(\text{H}_2)_{13}$ vibrational mode is markedly redshifted compared with pure H_2 and has different frequency behavior and broadening with pressure (see Fig. S1 [24]), which mirrors that of the HI vibron extremely closely. The similarities in the behavior of the two modes suggests strong intermolecular coupling between HI and H_2 . In the MD calculations we observe that the nearest approach between nonbonded H atoms involves the hydrogen in HI . Radial-distribution functions for H_2 molecules (see Fig. S2 [24]) also indicate the icosahedral symmetry adopted by the clusters and furthermore confirm that the $(\text{H}_2)_{13}$ supramolecular units are well separated and act as individual objects in the crystal structure. Changes in the average H-H bond distance with pressure (see Fig. S3 [24]) show no turnover in frequency, as is observed for pure H_2 over the same range, indicating marked changes in H_2 vibrational behavior in agreement with the strong intermolecular coupling observed in Raman spectra.

Another possible route to the synthesis of iodine-hydrogen compounds is by the compression of HI and H_2 , rather than I_2 and H_2 (Fig. 4). Mixtures of HI and H_2 were prepared at 0.2 GPa, where we observe clear phase separation between HI and H_2 . On compression above 0.3 GPa we observe the crystallization of HI phase I in the sample, which becomes grainy in texture [15]. At a pressure of 3.5 GPa, we observe the formation of large crystal grains as solid HI reacts with surrounding fluid H_2 . Diffraction peaks corresponding to the newly formed compound, hydrogen diiodane [$\text{H}_2(\text{HI})_2$], could be indexed to a body-centered-tetragonal unit cell $a = 7.8626(6)$ Å, $c = 6.5757(8)$ Å at 5 GPa. A complete systematic-absence analysis was not possible due to peak overlap with I_2 . However, the analogous $\text{H}_2(\text{H}_2\text{S})_2$ and $\text{H}_2(\text{CH}_4)_2$ compounds adopt space

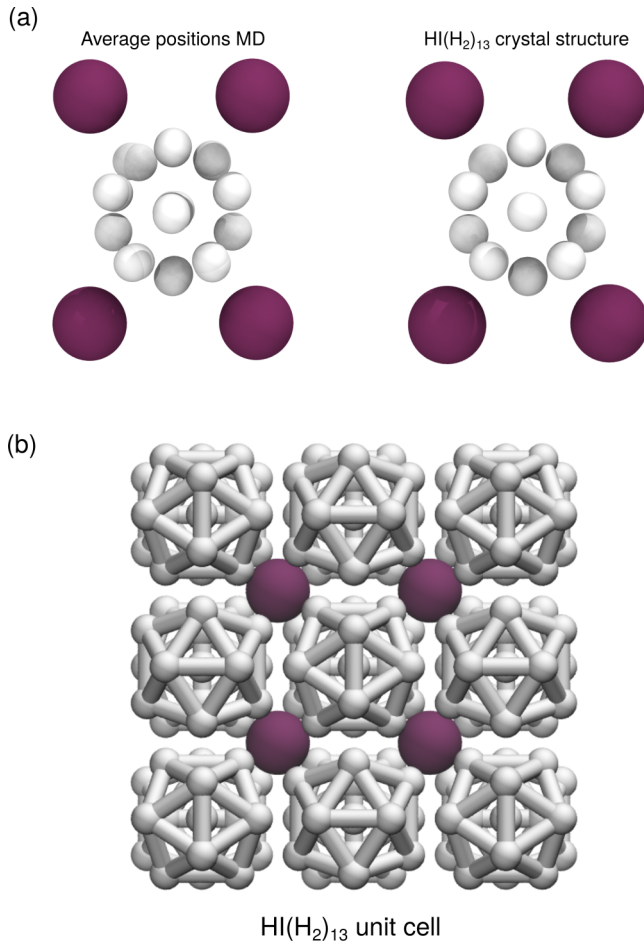


FIG. 3. Molecular dynamic trajectories and structural model of $\text{HI}(\text{H}_2)_{13}$. (a) Time-averaged mean positions of selected atoms from the MD trajectory viewed along (110). The mean position of either atom in a rotating diatomic molecule is at the molecular center, even though the atom is never actually there. Consequently, the H_2 molecules comprise two superimposed spheres, and only the iodine is visible for the HI molecules. (b) $(\text{H}_2)_{13}$ crystal structure with the orientation of icosahedral clusters highlighted with “bonds” between H_2 positions to guide the eye.

group $I4/mcm$, and subsequent refinement in this space group results in a good fit to the data with no unexplained peaks ($wR_p = 2.39\%$) [33,34]. In this structure, rotationally disordered HI molecules form alternating layers perpendicular to the c axis with H_2 molecules occupying vacancies between these layers.

Figure 2(c) shows the Raman spectra of hydrogen diiodane on compression. Below 3.5 GPa, only the vibrons of H_2 and HI phase I are observed. On compression to 3.5 GPa there is the appearance of a second H_2 vibron 90 cm^{-1} lower in frequency than that of the pure species. This mode softens with pressure, the opposite of pure molecular H_2 , which hardens in this pressure regime. The HI vibrational mode broadens slightly at the formation pressures; however, this was previously determined to be a transition to a phase I' in pure HI [15]. A combination of weak hydrogen bonding and decomposition means that, unlike $\text{H}_2(\text{H}_2\text{S})_2$, $\text{H}_2(\text{HI})_2$ does not undergo a H-ordering transition under compression but instead

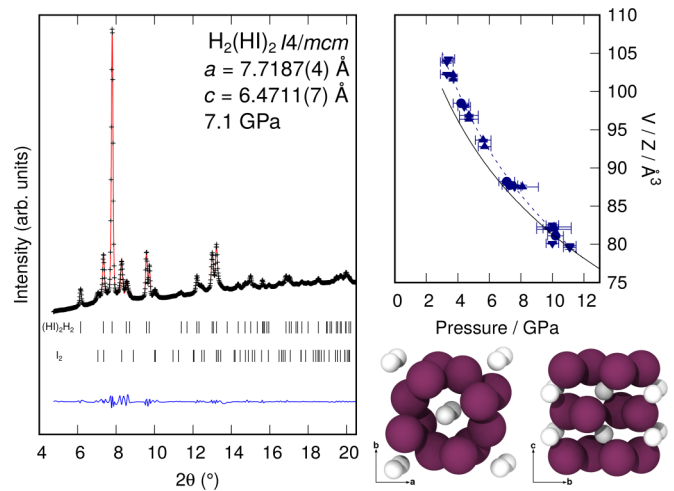


FIG. 4. X-ray diffraction structure analysis of $\text{H}_2(\text{HI})_2$. Left: High-pressure x-ray diffraction pattern of $\text{H}_2(\text{HI})_2$ at 7.1 GPa ($\lambda = 0.4141\text{ \AA}$), with the Le Bail profile refinement shown in red and difference shown in blue ($wR_p = 2.39\%$). Tick marks indicate Bragg peaks due to $(\text{HI})_2\text{H}_2$ and I_2 . Right: $\text{H}_2(\text{HI})_2$ equation of state. The dashed line corresponds to the fitted equation of state, and the solid line indicates the volume derived from the corresponding atomic equations of state of I_2 [11,27] and H_2 [28]. The volume per formula unit (V/Z) as a function of pressure shows good agreement with values calculated from the atomic equations of state for stoichiometry $\text{H}_2(\text{HI})_2$, supporting the result of the refinement. The crystal structure of $\text{H}_2(\text{HI})_2$ is body-centered-tetragonal with layers of HI molecules spaced along c by the insertion of H_2 . HI molecules are represented by purple spheres; H_2 molecules are shown by white spheres.

decomposes at slightly higher pressure (12.5 GPa) than pure HI (10 GPa) [15,33].

We observe diffraction peaks from $\text{HI}(\text{H}_2)_{13}$ (Raman vibrational modes were observed up to 58 GPa) over a remarkably large pressure range, from 9 GPa on decompression to 130 GPa on compression. Structural information obtained from x-ray diffraction can provide some indication as to the origin of this stability *versus* HI and $\text{H}_2(\text{HI})_2$. Amongst the hydrogen halides only HBr and HI have been experimentally proven to decompose into their constituent elements [15,35]. Previous molecular dynamics simulations of this process in HBr indicate that intermolecular distances reduce under compression, leading to the spontaneous formation of H_2 molecules [36]. Simulations have not yet been performed for HI; however, it seems likely that decomposition occurs in the same manner and requires the close approach of HI molecules before the formation of H_2 . Figure 1 shows the changes in $\text{I} \cdots \text{I}$ nearest and next-nearest distances with pressure for pure HI, $\text{H}_2(\text{HI})_2$, and $\text{HI}(\text{H}_2)_{13}$ derived from x-ray diffraction measurements. For HI and $\text{H}_2(\text{HI})_2$ nearest-neighbor distances are approximately equal, and both decrease rapidly with pressure before decomposition. The presence of additional layers of H_2 molecules along the c axis in $\text{H}_2(\text{HI})_2$ increases the next-nearest-neighbor distance relative to HI and may be responsible for the slightly higher stability of $\text{H}_2(\text{HI})_2$. Both cases contrast sharply with $\text{HI}(\text{H}_2)_{13}$, for which nearest-neighbor distances are just $0.58(3)\text{ \AA}$ shorter than the *interlayer* separation in $\text{H}_2(\text{HI})_2$ at 10.3 GPa (see inset in Fig. 1). It appears that isolating neighboring HI molecules from

each other in HI(H₂)₁₃ hinders the decomposition mechanism, stabilizing the compound by more than an order of magnitude. This remarkable change in stability makes HI(H₂)₁₃ among the most stable bimolecular compounds at high pressures, comparable to Xe(N₂)₂ and Xe(H₂)₈, which are stable up to 180 and 255 GPa, respectively [37,38]. Isolation also has a notable effect on the HI vibron frequency. In HI, like for the other hydrogen halides, the vibrational frequency is highly dependent upon the strength of the intermolecular interactions at a given temperature and pressure [39]. As pressure increases, intermolecular interactions increase in strength, weakening the covalent H-X bond and reducing vibrational frequency, as shown in Fig. 2(b). In the absence of the strong HI...HI intermolecular interactions characterizing the other phases, the HI vibron in HI(H₂)₁₃ has a significantly higher frequency [$\sim 2285\text{ cm}^{-1}$ at 13 GPa vs 1825 cm^{-1} at 9.8 GPa for H₂(HI)₂] and is much less pressure dependent.

IV. CONCLUSIONS

Triadecadihydrogen iodane has an unprecedented 93 mol % H₂ content. Among molecular hydrogen storage materials, HI(H₂)₁₃ shows a relatively high weight percent H₂ content, 17.7%, which compares favorably to other materials such as H₂(H₂O)₂ (5.3 H₂ wt %), H₂(H₂O) (11.2 H₂ wt %) [40], and Xe(H₂)₈ (10.9 H₂ wt %) [37], although it falls short of the record 33.4 wt % found in (H₂)₄CH₄ [40]. The formation of HI(H₂)₁₃ also poses an interesting question as to whether

such a structure could be stable for other molecules that satisfy a size ratio compatible with the (H₂)₁₃ supramolecular building block. Interestingly, Xe, isoelectronic to HI, has also been shown to form van der Waals compounds with H₂; it may be possible that higher-H₂-content structures could be stable in that system [37]. This observation of an AB₁₃ structure containing molecular hydrogen might initiate the search for molecules capable of forming such a hydrogen-rich stoichiometry at close to ambient pressures.

ACKNOWLEDGMENTS

The authors thank R. Hrubiak, S. Imada, and N. Hirao for their assistance during experiments. This work was supported by the NSF of China (Grant No. 11404343) and Natural Science Foundation of Anhui Province, China (Grant No. 1508085QA07). Part of this work was performed under Proposal No. 2017A1062 at SPring-8. Portions of this work were performed at HPCAT (Sector 16), Advanced Photon Source (APS), Argonne National Laboratory. HPCAT operations are supported by DOE-NNSA under Award No. DE-NA0001974, with partial instrumentation funding by NSF. The Advanced Photon Source is a US Department of Energy (DOE) Office of Science User Facility operated for the DOE Office of Science by Argonne National Laboratory under Contract No. DE-AC02-06CH11357. G.J.A. was supported by an ERC grant, “Hecate,” a Royal Society Wolfson Award. Computer time was provided by the UKCP consortium under EPSRC Grant No. EP/P022790.

-
- [1] E. Wigner and H. B. Huntington, *J. Chem. Phys.* **3**, 764 (1935).
 [2] M. I. Eremets and I. A. Troyan, *Nat. Mater.* **10**, 927 (2011).
 [3] P. Dalladay-Simpson, R. T. Howie, and E. Gregoryanz, *Nature (London)* **529**, 63 (2016).
 [4] X.-D. Liu, R. T. Howie, H.-C. Zhang, X.-J. Chen, and E. Gregoryanz, *Phys. Rev. Lett.* **119**, 065301 (2017).
 [5] M. D. Knudson, M. P. Desjarlais, A. Becker, R. W. Lemke, K. R. Cochrane, M. E. Savage, D. E. Bliss, T. R. Mattsson, and R. Redmer, *Science* **348**, 1455 (2015).
 [6] V. V. Struzhkin, B. Militzer, W. L. Mao, H.-k. Mao, and R. J. Hemley, *Chem. Rev.* **107**, 4133 (2007).
 [7] N. L. Rosi, J. Eckert, M. Eddaoudi, D. T. Vodak, J. Kim, M. O’Keeffe, and O. M. Yaghi, *Science* **300**, 1127 (2003).
 [8] M. P. Suh, H. J. Park, T. K. Prasad, and D.-w. Lim, *Chem. Rev.* **112**, 782 (2012).
 [9] A. P. Drozdov, M. I. Eremets, I. A. Troyan, V. Ksenofontov, and S. I. Shylin, *Nature (London)* **525**, 73 (2015).
 [10] A. S. Balchan and H. G. Drickamer, *J. Chem. Phys.* **34**, 1948 (1961).
 [11] R. Reichlin, A. K. McMahan, M. Ross, S. Martin, J. Hu, R. J. Hemley, H.-k. Mao, and Y. Wu, *Phys. Rev. B* **49**, 3725 (1994).
 [12] T. Kenichi, S. Kyoko, F. Hiroshi, and O. Mitsuko, *Nature (London)* **423**, 971 (2003).
 [13] A. Shamp and E. Zurek, *J. Phys. Chem. Lett.* **6**, 4067 (2015).
 [14] D. Duan, F. Tian, Y. Liu, X. Huang, D. Li, H. Yu, Y. Ma, B. Liu, and T. Cui, *Phys. Chem. Chem. Phys.* **17**, 32335 (2015).
 [15] J. Binns, X.-D. Liu, P. Dalladay-Simpson, V. Afonina, E. Gregoryanz, and R. T. Howie, *Phys. Rev. B* **96**, 144105 (2017).
 [16] A. N. Jackson and G. J. Ackland, *Phys. Rev. E* **76**, 066703 (2007).
 [17] H. K. Mao, J. Xu, and P. M. Bell, *J. Geophys. Res.* **91**, 4673 (1986).
 [18] Y. Fei, A. Ricolleau, M. Frank, K. Mibe, G. Shen, and V. Prakapenka, *Proc. Natl. Acad. Sci. USA* **104**, 9182 (2007).
 [19] Y. Akahama and H. Kawamura, *J. Phys. Conf. Ser.* **215**, 12195 (2010).
 [20] C. Prescher and V. B. Prakapenka, *High Pressure Res.* **35**, 223 (2015).
 [21] V. Petříček, M. Dušek, and L. Palatinus, *Z. Kristallogr. Cryst. Mater.* **229**, 345 (2014).
 [22] G. M. Sheldrick, *Acta Crystallogr., Sect. C* **71**, 3 (2015).
 [23] S. J. Clark, M. D. Segall, C. J. Pickard, P. J. Hasnip, M. J. Probert, K. Refson, and M. Payne, *Z. Kristallogr.* **220**, 567 (2005).
 [24] See Supplemental Material at <http://link.aps.org/supplemental/PhysRevB.97.024111> for the experimental details.
 [25] T. Scheler, M. Marqués, Z. Konopkova, C. L. Guillaume, R. T. Howie, and E. Gregoryanz, *Phys. Rev. Lett.* **111**, 215503 (2013).
 [26] C. M. Pépin, G. Geneste, A. Dewaele, M. Mezouar, and P. Loubeyre, *Science* **357**, 382 (2017).
 [27] K. Takemura, S. Minomura, O. Shimomura, Y. Fujii, and J. D. Axe, *Phys. Rev. B* **26**, 998 (1982).
 [28] P. Loubeyre, R. LeToullec, D. Hausermann, M. Hanfland, R. J. Hemley, H.-k. Mao, and L. W. Finger, *Nature (London)* **383**, 702 (1996).
 [29] N. Baenziger and R. Rundle, *Acta Crystallogr.* **2**, 258 (1949).

- [30] A. B. Schofield, P. N. Pusey, and P. Radcliffe, *Phys. Rev. E* **72**, 031407 (2005).
- [31] M. J. Murray and J. V. Sanders, *Philos. Mag. A* **42**, 721 (1980).
- [32] A. Anderson, B. H. Torrie, and W. S. Tse, *J. Raman Spectrosc.* **8**, 213 (1979).
- [33] T. A. Strobel, P. Ganesh, M. Somayazulu, P. R. C. Kent, and R. J. Hemley, *Phys. Rev. Lett.* **107**, 255503 (2011).
- [34] M. Somayazulu, L. W. Finger, R. J. Hemley, and H. K. Mao, *Science* **271**, 1400 (1996).
- [35] T. Kume, T. Tsuji, S. Sasaki, and H. Shimizu, *Phys. Rev. B* **58**, 8149 (1998).
- [36] T. Ikeda, M. Sprik, K. Terakura, and M. Parrinello, *Phys. Rev. Lett.* **81**, 4416 (1998).
- [37] M. Somayazulu, P. Dera, A. F. Goncharov, S. A. Gramsch, P. Liermann, W. Yang, Z. Liu, H.-k. Mao, and R. J. Hemley, *Nat. Chem.* **2**, 50 (2009).
- [38] R. T. Howie, R. Turnbull, J. Binns, M. Frost, P. Dalladay-Simpson, and E. Gregoryanz, *Sci. Rep.* **6**, 34896 (2016).
- [39] W. Y. Zeng, Y. Z. Mao, and A. Anderson, *J. Raman Spectrosc.* **30**, 995 (1999).
- [40] W. L. Mao and H.-k. Mao, *Proc. Natl. Acad. Sci. USA* **101**, 708 (2004).